


ORIGINAL ARTICLE

Open Access



Pathology and genetic connectedness of the mangrove crab (*Aratus pisonii*) – a foundation for understanding mangrove disease ecology

Jamie Bojko^{1,2*} , Amy L. Burgess^{1,2}, Thomas W. Allain^{3,4}, Erica P. Ross⁵, Devon Pharo⁵, Jan F. Kreuze⁶ and Donald C. Behringer^{3,4}

Abstract

Mangrove forests are productive ecosystems, acting as a sink for CO₂, a habitat for a diverse array of terrestrial and marine species, and as a natural barrier to coastline erosion. The species that reside within mangrove ecosystems have important roles to play, including litter decomposition and the recycling of nutrients. Crustacea are important detritivores in such ecosystems and understanding their limitations (i.e. disease) is an important endeavour when considering the larger ecological services provided.

Histology and metagenomics were used to identify viral (*Nudiviridae*, *Alphaflexiviridae*), bacterial (*Paracoccus* sp., '*Candidatus* *Gracilibacteria* sp.', and *Pseudoalteromonas* sp.), protozoan, fungal, and metazoan diversity that compose the symbiome of the mangrove crab, *Aratus pisonii*. The symbiotic groups were observed at varying prevalence under histology: nudivirus (6.5%), putative gut epithelial virus (3.2%), ciliated protozoa (35.5%), gonad fungus (3.2%), gill ectoparasitic metazoan (6.5%). Metagenomic analysis of one specimen exhibiting a nudivirus infection provided the complete host mitochondrial genome (15,642 bp), nudivirus genome (108,981 bp), and the genome of a Cassava common mosaic virus isolate (6387 bp). Our phylogenetic analyses group the novel nudivirus with the *Gammanudivirus* and protein similarity searches indicate that *Carcinus maenas* nudivirus is the most similar to the new isolate. The mitochondrial genome were used to mine short fragments used in population genetic studies to gauge an idea of diversity in this host species across the USA, Caribbean, and central and southern America. This study report several new symbionts based on their pathology, taxonomy, and genomics (where available) and discuss what effect they may have on the crab population. The role of mangrove crabs from a OneHealth perspective were explored, since their pathobiome includes cassava-infecting viruses. Finally, given that this species is abundant in mangrove forests and now boasts a well-described pathogen profile, we posit that *A. pisonii* is a valuable model system for understanding mangrove disease ecology.

Keywords: *Alphaflexiviridae*, *Nudiviridae*, Mitochondria, Pathology, Histology, Metagenomics

* Correspondence: J.Bojko@tees.ac.uk

²School of Health and Life Sciences, Teesside University, Middlesbrough TS1 3BX, UK

Full list of author information is available at the end of the article



© The Author(s). 2022 **Open Access** This article is licensed under a Creative Commons Attribution 4.0 International License, which permits use, sharing, adaptation, distribution and reproduction in any medium or format, as long as you give appropriate credit to the original author(s) and the source, provide a link to the Creative Commons licence, and indicate if changes were made. The images or other third party material in this article are included in the article's Creative Commons licence, unless indicated otherwise in a credit line to the material. If material is not included in the article's Creative Commons licence and your intended use is not permitted by statutory regulation or exceeds the permitted use, you will need to obtain permission directly from the copyright holder. To view a copy of this licence, visit <http://creativecommons.org/licenses/by/4.0/>. The Creative Commons Public Domain Dedication waiver (<http://creativecommons.org/publicdomain/zero/1.0/>) applies to the data made available in this article, unless otherwise stated in a credit line to the data.

Introduction

Mangrove forests are some of the world's most productive ecosystems (Sandilyan and Kathiresan 2012), growing at the vegetation boundary between land and sea, and line ~70% of tropical coasts (Conde et al. 2000; Rogers et al. 2021). This unique ecosystem provides refuge for a diverse array of invertebrate species (Sandilyan and Kathiresan 2012). Across the broad diversity of inhabitants, mangrove crabs are an important keystone group (Smith III et al. 1991; Conde et al. 2000). *Aratus pisonii*, the neotropical mangrove crab, inhabits the supralittoral zone of multiple mangrove species (*Rhizophora mangle*; *Avicennia germinans*; *Laguncularia racemosa*; *Pelliceria rhizophorae*) (Díaz and Conde 1989; Conde et al. 2000). Its distribution ranges from Eastern Florida to Northern Brazil, including the Caribbean, as well as between Nicaragua and Peru on the Pacific Coast. The habitat range is thought to be under expansion, responding to a warming climate (Riley et al. 2014).

Data pertaining to mangrove ecologies often lack the important factor of disease prevalence and distribution, including the exploration and ecological perception of how parasites and pathogens contribute to the natural functioning of an ecological system (i.e., Disease Ecology). Such concepts are vital since changes in disease occurrence or prevalence can profoundly alter the species composition of an ecosystem. For example, the lack of a disease can cause certain species to over-compete (Strauss et al. 2019) or disease outbreaks can cause trophic cascades and change community composition (Behrens and Lafferty 2004). To date, the mangrove crab, *A. pisonii*, is associated with few parasitic groups, restricted only to fungal observations by Mattson (Mattson 1988), where Eccrinaceous fungi (Trichomycetes) were observed in the hindgut of *A. pisonii* from Tampa Bay, Florida. These fungal observations were quantitatively associated with the crab's detritivorous and herbivorous diet. Considering this species is a keystone element of mangrove forests, with an ecological role disproportionately large relative to its abundance, it is pertinent to explore any associated diseases, such as viral, bacterial, and other microparasitic groups.

The availability of novel genetic and genomic technologies allowed us to better map and describe the associated pathobiome of animals and plants (Bass et al. 2019). An added benefit to such technology is the additional genetic information gained from the host organism. Mitochondrial genetic data has been collected for *A. pisonii* across its range, outlining some haplotype variation that deserves further exploration (Riley and Griffen 2017; NCBI). Of benefit to pathological understanding, techniques such as histology provide a method to generally screen for parasite groups, allowing one to find a pathology of interest and then follow-up with

more accurate tools to provide taxonomic detail (Bojko et al. 2017; Warren et al. 2022).

Using histopathological and metagenomic technology, we provide an up to date understanding of the virology, bacteriology, and general parasitology of *A. pisonii* from the Florida Keys, while providing an additional series of genetic resources and community analysis for this host species, including the mitochondrial genome. The availability of such data brings this species forward as an intriguing disease ecology model for understanding the role of disease in mangrove ecosystems.

Results

Histopathology

Five different symbiotic groups were identified histologically, including gill ectoparasitic organisms (Fig. 1A), ciliated protozoans (Fig. 1B), gonad-infecting fungi (Fig. 1C-D), a nudivirus (Fig. 1E) and a putative epithelial virus (Fig. 1F-G). Ectoparasitic organisms were observed between the gill lamellae of 2/31 (6.5%) hosts, with distinguishable muscle, nerve and gonad tissue (Fig. 1A). Ciliated protozoans were also observed between the gill lamellae of the host (11/31; 35.5%), consisting of basophilic staining ciliates with U-shaped nuclei (Fig. 1B) – in some cases the ciliates were stalked. A single animal was infected with a fungal parasite observable in the male gonad (1/31; 3.2%) (Fig. 1C). High magnification images of the infection revealed a network of hyphal-like strands extending into the host testes (Fig. 1D). A novel nudivirus was noted to produce a basophilic viroplasm that resulted in nuclear hypertrophy in affected hepatopancreocytes in 2/31 (6.5%) hosts, which also displayed an eosinophilic staining occlusion (resembling a thin red shard) as well as causing margination of host chromatin (Fig. 1E). The host hepatopancreas housing this virus was further analysed using metagenomics outlined below. Finally, an eosinophilic shard, similar to that seen in the hepatopancreas of the crabs infected with the nudivirus, was also present in the nuclei of host gut epithelia in one crab (1/31; 3.2%); however, the crab with this infection did not have the nudiviral pathology. Gut material was not preserved in ethanol and no further confirmation of this putative viral pathology could be conducted with the material available.

Cassava common mosaic virus (Alphaflexiviridae) and Nudiviridae in a mangrove crab

One contiguous sequence mined from the metagenomic data (acquired from host hepatopancreas DNA extract) (1678 bp, X7 coverage) represented the 18S gene of *Manihot esculenta* (Cassava) (XR_006349510: coverage: 99%, similarity 99.4%, e-value: 0.0), the primary host of Cassava common mosaic virus (CsCMV). In addition, a second contiguous DNA sequence conferred to the

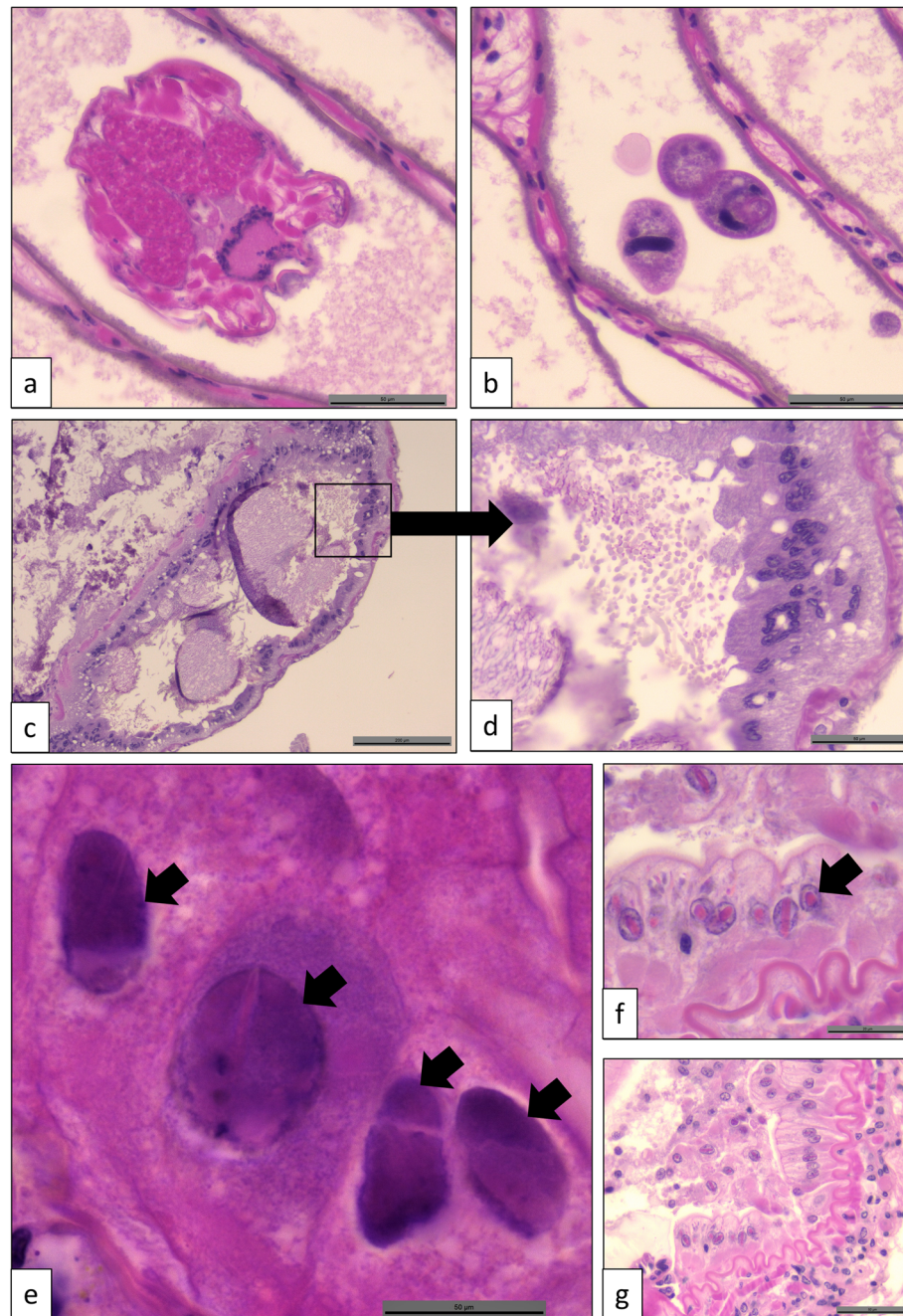


Fig. 1 Histopathology of *Aratus pisonii* collected from the Florida Keys. **A** A gill-based ectoparasite including a transverse section through the middle of the animal, likely Polychaeta. **B** Ciliated protozoa sitting between the gill lamellae. **C-D** A network of fungal hyphae in the male gonad. **E** Nudivirus-infected nuclei of hepatopancreatocytes. **F-G** Putative gut-infection consisting of virally infected gut-epithelial nuclei

complete genome of the RNA virus CsCMV (6387 bp, X49 coverage) (Fig. 2; Table 1). The sequence of the new isolate included all the expected proteins and showed high similarity at both the protein and genetic scale (Table 1). Phylogenetic comparison to other CsCMV isolates places this new isolate as an early diverging strain when comparing complete genome data (Fig. 2). Phylogenetic comparison of the replicase and capsid

proteins among strains confirmed on both occasions that the more similar strain was CsCMV strain Arg127 (KT002439), from Argentina. The novel isolate is stored in GenBank under accession: OM927720.

The metagenomic data also included a complete, circular, genome corresponding to the *Nudiviridae* (108,981 bp, X158 coverage). The genome included 91 protein coding genes, with all expected conserved genes

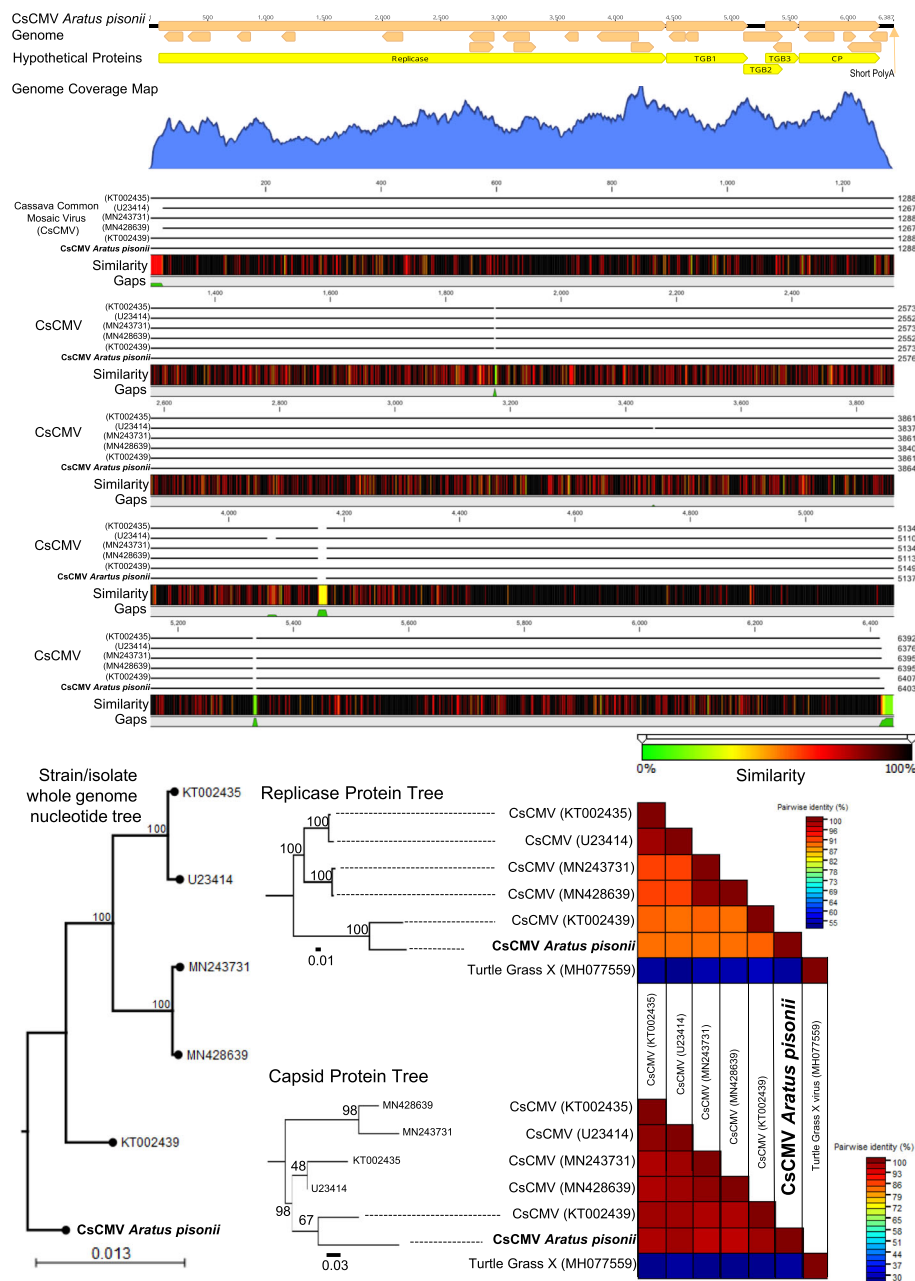


Fig. 2 Genomic annotation and similarity assessment of a novel Cassava Common Mosaic Virus (CsCMV) strain, mined from the *Aratus pisonii* metagenome data. The viral genome was identified from DNA data, suggesting it was reverse transcribed in the host cell. The genome represents all five of the open reading frames common to CsCMV, along with a short PolyA tail. Single nucleotide polymorphism comparison across the genome is presented, ranging from green (dissimilar) to black (similar). Whole genome nucleotide phylogenetics, replicase protein phylogenetics and capsid protein phylogenetics are present, as well as a pairwise comparison of both the replicase and capsid proteins across the strains. Graphics developed in CLC genomics workbench V. 20. Phylogenetic trees developed in IQtree. Similarity tables developed using Sequence Demarcation Tool V. 1.2

(Fig. 3; Table 2). The highest protein similarity, including lowest e-values, between existing *Nudiviridae* and the new isolate was represented by similarity to *Carcinus maenas* nudivirus (CmNV) (44/91 genes), *Homarus gammarus* nudivirus (HgNV) (27/91 genes), *Penaeus monodon* nudivirus (PmNV) (4/91), *Dikerogammarus*

haemobaphes nudivirus (DhNV) (1/91), and *Macrobrachium rosenbergii* nudivirus (MrNV) (1/91) (Table 2). Two proteins showed some similarity to proteins encoded by decapods, including a serine/threonine kinase (ApNV_020) (*Homarus americanus*, 30.1%, $4e-10$) and 'GWK47_016212' (ApNV_043) (*Chionoecetes opilio*,

Table 1 *Alphaflexiviridae* nucleotide and protein similarity table, determined using BLASTn and BLASTp

Genetic region/protein	Hit (accession)	Coverage (%)	Similarity (%)	E-value
Whole genome (nucleotide)	Cassava common mosaic virus isolate Hainan-CM (MW175326)	99	98.5	0.0
Replicase (protein)	Cassava common mosaic virus (QJ539010)	100	98.4	0.0
TGB1 (protein)	Cassava common mosaic virus (QIA16092)	100	96.5	2e-166
TGB2 (protein)	Cassava common mosaic virus (QKG28055)	100	95.5	1e-70
TGB3 (protein)	Cassava common mosaic virus (QKG28056)	100	96.8	1e-57
Capsid (protein)	Cassava common mosaic virus (QKG28057)	100	97.3	2e-162

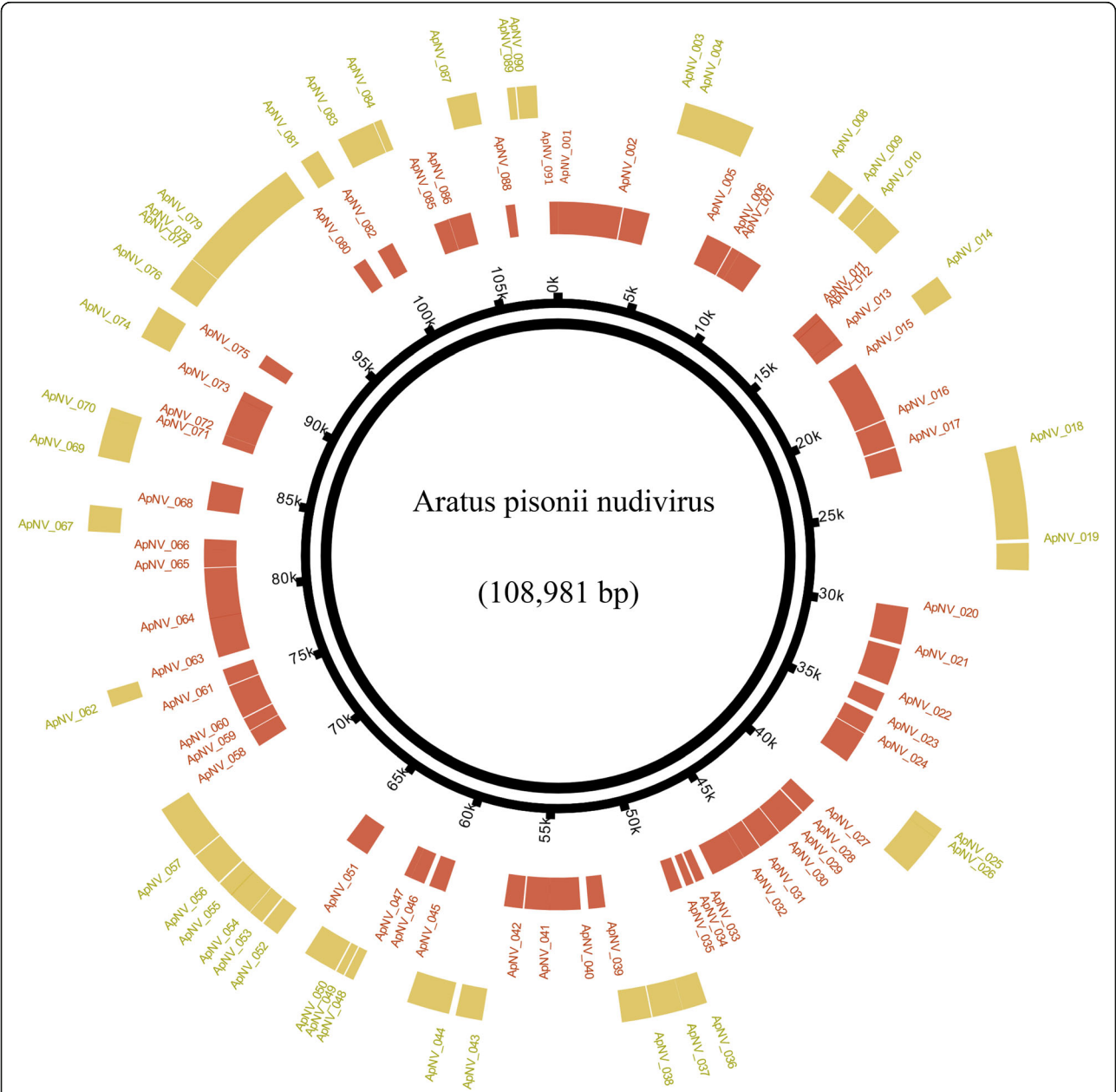


Fig. 3 *Aratus pisonii* nudivirus (ApNV) genome plot, highlighting negative strand (gold) and positive strand (red) protein coding genes. The ApNV number is listed in the appropriate colour according to the gene it represents and the strand it is present on. The figure was developed using CIRCA

Table 2 'Aratus pisonii nudivirus' (ApNV) protein similarity table. Similarity and function/domain are determined using BLASTp

ORF	Strand	Left End	Right End	Gene Length (nt)	Protein hit (virus: accession)	Similarity (%)	Coverage (%)	E-value
ApNV_001	+	1	3177	3177	DNA pol (HgNV: YP_010087641)	56.9	99	0.0
ApNV_002	+	3244	4542	1299	methylytransferase (CmNV: UBZ25592)	39.7	91	1e-78
ApNV_003	–	4752	5411	660	Ac92-like protein (CmNV: UBZ25594)	52.3	88	1e-70
ApNV_004	–	5408	7432	2025	Vp91 (CmNV: UBZ25595)	45.1	99	0.0
ApNV_005	+	7544	8857	1314	ODV-E56 (HgNV: YP_010087646)	55.6	95	2e-159
ApNV_006	+	8916	9350	435	KM727_gp07 (HgNV: YP_010087647)	44.1	99	6e-35
ApNV_007	+	9350	10,585	1236	P47 (CmNV: UBZ25598)	51.2	98	6e-138
ApNV_008	–	10,610	11,746	1137	PIF-2 (CmNV: UBZ25599)	64.4	98	5e-177
ApNV_009	–	12,012	12,764	753	p-loop NTPase/TK1 (PmNV: YP_009051855)	30.8	74	4e-22
ApNV_010	–	12,808	14,073	1266	CmNV_011 (CmNV: UBZ25601)	33.2	83	9e-50
ApNV_011	+	14,160	14,534	375	CmNV_012 (CmNV: UBZ25602)	33.3	97	1e-10
ApNV_012	+	14,507	15,742	1236	FEN-1 (CmNV: UBZ25603)	43.2	98	5e-108
ApNV_013	+	15,726	16,202	477	KM727_gp14 (HgNV: YP_010087654)	38.0	98	1e-26
ApNV_014	–	16,235	17,179	945	31 k virion structural protein (CmNV: UBZ25605)	44.1	92	1e-80
ApNV_015	+	17,297	20,362	3066	LEF-8 (HgNV: YP_010087656)	60.6	99	0.0
ApNV_016	+	20,428	21,774	1347	Hypothetical protein (no similarity)	–	–	–
ApNV_017	+	21,860	23,062	1203	P51 (HgNV: YP_010087657)	40.5	95	1e-105
ApNV_018	–	23,147	26,620	3474	CmNV_018 (CmNV: UBZ25608)	40.0	58	3e-140
ApNV_019	–	26,760	27,779	1020	E3 ubiquitin-protein ligase TRIM39-like protein (HgNV: YP_010087659)	25.8	36	9e-06
ApNV_020	+	29,791	31,632	1842	Serine/Threonine kinase (<i>Homarus americanus</i> : XP_042227734)	30.1	23	4e-10
ApNV_021	+	31,845	33,719	1875	ODV-E66 (PmNV: YP_009051874)	52.9	98	0.0
ApNV_022	+	34,155	35,114	960	Hypothetical protein (no similarity)	–	–	–
ApNV_023	+	35,420	36,337	918	TK2 (CmNV: UBZ25616)	44.8	100	9e-86
ApNV_024	+	36,377	37,972	1596	PIF-1 (CmNV: UBZ25617)	55.9	99	0.0
ApNV_025	–	37,969	38,385	417	Hypothetical protein (no similarity)	–	–	–
ApNV_026	–	38,375	39,979	1605	CmNV_029 (CmNV: UBZ25619)	48.2	99	7e-159
ApNV_027	+	40,471	41,232	762	KM727_gp31 (HgNV: YP_010087671)	41.2	94	1e-56
ApNV_028	+	41,307	42,047	741	KM727_gp32 (HgNV: YP_010087672)	38.1	91	9e-36
ApNV_029	+	42,040	42,765	726	PmV-like protein (CmNV: UBZ25622)	50.6	97	5e-81
ApNV_030	+	42,808	43,944	1137	p-loop NTPase (HgNV: YP_010087674)	44.4	97	3e-100
ApNV_031	+	43,990	44,904	915	CmNV_034 (CmNV: UBZ25624)	40.7	99	2e-71
ApNV_032	+	44,910	46,655	1746	CmNV_035 (CmNV: UBZ25625)	40.0	100	6e-128
ApNV_033	+	47,110	47,559	450	LEF-5 (CmNV: UBZ25628)	40.2	78	2e-19
ApNV_034	+	47,674	48,069	395	Predicted p6.9 (no similarity)	–	–	–
ApNV_035	+	48,280	48,903	624	CmNV_039 (CmNV: UBZ25630)	41.7	95	3e-36
ApNV_036	–	48,910	49,830	921	Integrase (CmNV: UBZ25631)	56.7	97	3e-122
ApNV_037	–	49,834	50,979	1146	HgNV_071-like (DhNV: QLI62437)	26.7	90	5e-19
ApNV_038	–	51,025	52,131	1107	LOC108666550-like protein (HgNV: YP_010087711)	23.1	93	9e-19
ApNV_039	+	52,162	52,998	837	VLF-1 (HgNV: YP_010087683)	44.7	98	3e-77
ApNV_040	+	53,378	54,919	1542	Hypothetical protein (no similarity)	–	–	–
ApNV_041	+	54,912	56,147	1236	Hypothetical protein (no similarity)	–	–	–

Table 2 'Aratus pisonii nudivirus' (ApNV) protein similarity table. Similarity and function/domain are determined using BLASTp
(Continued)

ORF	Strand	Left End	Right End	Gene Length (nt)	Protein hit (virus: accession)	Similarity (%)	Coverage (%)	E-value
ApNV_042	+	56,229	57,155	927	Hypothetical protein (no similarity)	–	–	–
ApNV_043	–	57,302	58,303	1002	GWK47_016212 (<i>Chionoecetes opilio</i> : KAG0713444)	34.9	70	8e-25
ApNV_044	–	58,551	60,155	1605	LEF-9 (CmNV: UBZ25637)	62.3	93	0.0
ApNV_045	+	60,110	60,955	846	38 K protein (HgNV: YP_010087687)	45.1	94	2e-68
ApNV_046	+	61,220	61,939	720	CmNV_049 (CmNV: UBZ25640)	41.9	97	3e-54
ApNV_047	+	61,936	62,289	354	PmNV_062 (PmNV: YP_009051900)	38.8	99	1e-20
ApNV_048	–	62,298	62,648	351	CmNV_051 (CmNV: UBZ25642)	37.4	78	2e-12
ApNV_049	–	62,699	62,998	300	CmNV_052 (CmNV: UBZ25643)	36.6	52	4e-08
ApNV_050	–	63,057	64,334	1278	TK1 (CmNV: UBZ25644)	43.4	100	4e-113
ApNV_051	+	64,365	65,594	1230	KM727_gp54 (HgNV: YP_010087694)	41.8	84	4e-89
ApNV_052	–	65,569	66,228	660	CmNV_058 (CmNV: UBZ25649)	33.7	90	2e-25
ApNV_053	–	66,297	66,860	564	KM727_gp58 (HgNV: YP_010087698)	43.0	99	1e-45
ApNV_054	–	66,878	67,813	936	CmNV_060 (CmNV: UBZ25651)	40.5	95	7e-77
ApNV_055	–	67,783	68,391	609	CmNV_061 (CmNV: UBZ25652)	48.2	94	9e-59
ApNV_056	–	68,454	69,740	1287	KM727_gp61 (HgNV: YP_010087701)	30.0	98	3e-57
ApNV_057	–	69,788	71,869	2082	PIF-0 (CmNV: UBZ25654)	61.7	98	0.0
ApNV_058	+	71,907	72,770	864	Zonadhesin (PmNV: YP_009051911)	27.7	49	0.048
ApNV_059	+	72,803	73,444	642	KM727_gp65 (HgNV: YP_010087705)	27.2	59	4e-04
ApNV_060	+	73,505	75,187	1683	Helicase 2 (CmNV: UBZ25657)	52.7	99	0.0
ApNV_061	+	75,239	76,069	831	Hypothetical protein (no similarity)	–	–	–
ApNV_062	–	76,066	76,707	642	KM727_gp68 (HgNV: YP_010087708)	43.6	98	2e-47
ApNV_063	+	76,697	78,643	1947	Helicase 2 (HgNV: YP_010087709)	49.5	88	1e-172
ApNV_064	+	78,622	81,132	2511	CmNV_070 (CmNV: UBZ25661)	28.4	71	7e-34
ApNV_065	+	81,171	82,055	885	CmNV_071 (CmNV: UBZ25662)	40.6	98	1e-62
ApNV_066	+	82,046	82,570	525	Hypothetical protein (no similarity)	–	–	–
ApNV_067	–	82,646	83,629	984	Hypothetical protein (no similarity)	–	–	–
ApNV_068	+	83,997	85,418	1422	Hypothetical protein (no similarity)	–	–	–
ApNV_069	–	85,433	86,920	1488	KM727_gp74 (HgNV: YP_010087714)	23.2	96	9e-31
ApNV_070	–	86,914	87,309	396	KM727_gp75 (HgNV: YP_010087715)	42.8	98	3e-30
ApNV_071	+	87,299	87,781	483	Ac81-like protein (HgNV: YP_010087716)	60.4	99	7e-67
ApNV_072	+	87,784	89,688	1905	CmNV_076 (CmNV: UBZ25667)	36.8	98	4e-117
ApNV_073	+	89,675	90,106	432	PIF-6 (CmNV: UBZ25668)	57.3	100	9e-58
ApNV_074	–	90,118	91,407	1290	KM727_gp79 (HgNV: YP_010087719)	36.6	85	3e-78
ApNV_075	+	91,492	92,208	717	VLF-1 (CmNV: UBZ25670)	49.0	99	1e-62
ApNV_076	–	92,198	93,553	1356	LEF-4 (CmNV: UBZ25671)	43.9	96	6e-123
ApNV_077	–	93,574	93,891	318	CmNV_081 (CmNV: UBZ25672)	45.2	88	6e-25
ApNV_078	–	93,888	94,481	594	PIF-3 (CmNV: UBZ25673)	63.6	93	2e-90
ApNV_079	–	94,478	98,290	3813	Helicase (CmNV: UBZ25674)	48.9	98	0.0
ApNV_080	+	98,292	98,987	696	PIF-4 (CmNV: UBZ25675)	54.4	96	2e-82
ApNV_081	–	98,956	99,708	753	KM727_gp86 (HgNV: YP_010087726)	39.7	96	3e-59
ApNV_082	+	99,707	100,534	828	Esterase (HgNV: YP_010087727)	56.0	90	3e-95
ApNV_083	–	100,548	101,981	1434	GbNV_gp67-like protein (CmNV: UBZ25678)	51.9	33	1e-48

Table 2 'Aratus pisonii nudivirus' (ApNV) protein similarity table. Similarity and function/domain are determined using BLASTp (Continued)

ORF	Strand	Left End	Right End	Gene Length (nt)	Protein hit (virus: accession)	Similarity (%)	Coverage (%)	E-value
ApNV_084	–	102,008	102,313	306	11 K (MrNV: UHB41834)	67	93	1e-44
ApNV_085	+	102,770	103,534	765	CmNV_090 (CmNV: UBZ25681)	38.0	97	2e-59
ApNV_086	+	103,544	104,650	1107	Apoptosis inhibitor (CmNV: UBZ25682)	29.6	93	7e-45
ApNV_087	–	104,835	105,953	1119	IAP (CmNV: UBZ25648)	32.4	46	5e-25
ApNV_088	+	106,393	106,860	468	Hypothetical protein (no similarity)	–	–	–
ApNV_089	–	107,090	107,398	309	Hypothetical protein (no similarity)	–	–	–
ApNV_090	–	107,451	108,188	738	CmNV_097 (CmNV: UBZ25688)	61.5	95	3e-107
ApNV_091	+	108,553	108,981	429	KM727_gp97 (HgNV: YP_010087737)	41.9	95	3e-29

34.9%, 8e-25). The remaining 12 genes showed no similarity to other viral (or other organism) sequences in the GenBank database and their function remains unpredicted.

A multi-gene phylogeny consisting of 17 single copy conserved genes, including the new virus and other representative *Nudiviridae*, determined that ApNV groups within the *Gammanudivirus* genus most closely to PmNV, HgNV, and CmNV (bootstrap confidence: 100) (Fig. 4). A single-gene tree using all available DNA polymerase protein sequences for the *Nudiviridae* also placed the new virus in the same topological position. The novel isolate is stored in GenBank under accession: ON061174.

Metaxa2 results – eukaryotic and bacterial symbiont diversity

The metaxa2 results, which involved mining the assembled metagenomic data from the host hepatopancreas for SSU and LSU sequences resulted in no eukaryotic sequences outside of the host (*Aratus*) or plant. Eight relatively low-coverage sequences referred to several bacterial associations in the host hepatopancreas (Table 3). Most results showed greatest similarity to bacterial clones from other metagenomic studies including: the microbiome of *Palinurid phyllosoma* (Payne et al. 2008); bacterial symbionts of *Artemia* spp. in Israel (Tkavc et al. 2011); gut microbiome of *Eriocheir sinensis* (Chen et al. 2015); and bacteria from ground water (Luef et al. 2015). *Paracoccus* sp. (88.6% similarity), '*Candidatus* Gracilibacteria sp.' (90.5% similarity), and *Pseudoalteromonas* sp. (96.5% similarity) were the most discernible taxonomically identified genera (Table 3). The sequence data are stored under accession numbers: ON063416-ON063422.

Genetic data for *Aratus pisonii*

The mitochondrial genome of *A. pisonii* is a closed circular molecule of 15,642 bp (X98 coverage) (accession: OM935816). The mitochondrial genome encodes 13

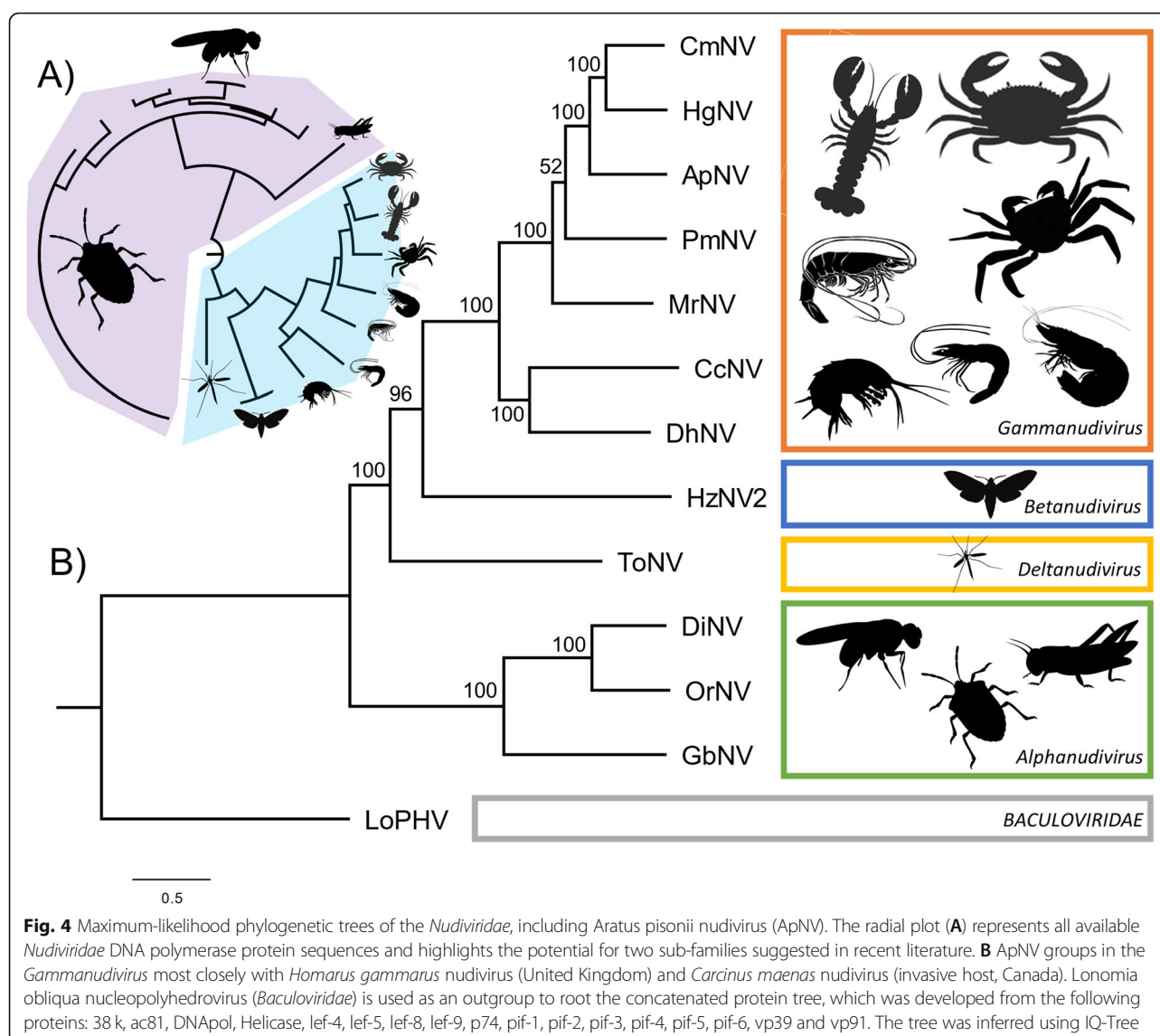
protein coding genes, 22 tRNAs and 2 rRNAs. A single control region is also present (CoRe). *Aratus pisonii* exhibits the SesGO gene order shown in Fig. 5 (Basso et al. 2017). The protein coding regions encompass 7 NADH dehydrogenases (*nad1-nad6*, *nad4L*), three cytochrome c oxidases (*cox1-cox3*), 2 ATPases (*atp6* and *atp8*) and 1 cytochrome b (*cob*). All the protein coding genes, including a high proportion of the non-coding RNA genes (ncRNA), showed a high level of similarity with other crabs belonging to the Sesarmidae family (Additional file 1).

To establish where *A. pisonii* aligned within the Sesarmidae family, *cox1* nucleotide sequences from 20 species across the Brachyura: 15 genera from five families. The Sesarmidae family formed a distinct clade. The mangrove crab forms a new branch for *Aratus* (bootstrap: 98). *Chiramantes* appears to be polyphyletic, *Chiramantes dehanni* aligns with *Sesarma neglectum* (bootstrap: 100) whilst *C. haematocheir* aligns with *Sesarmops sinensis* (bootstrap: 100) (Fig. 5).

The two haplotype networks generated in this study indicate that high levels of genetic divergence exist amongst *A. pisonii* populations throughout the Americas and the Caribbean (Fig. 6). The star-like groupings present across both networks are evidence of haplotype structuring (Fig. 6B). The *cox1* network has star-like groupings restricted to individual geographic regions, with relate to rare haplotypes projecting from more frequent ones.

Discussion

The population structure of *A. pisonii*, inferred from the haplotype networks, suggests the formation of four regional haplotypes: North America, Central America, the Caribbean, and South America. This genetic population structure may result from the high dispersive potential of the mangrove tree crab and barriers to gene flow that arise from the mangrove and marine environment. The genetic structure seen here is supported by previous phylogeographic study of the mangrove crab (Buranelli

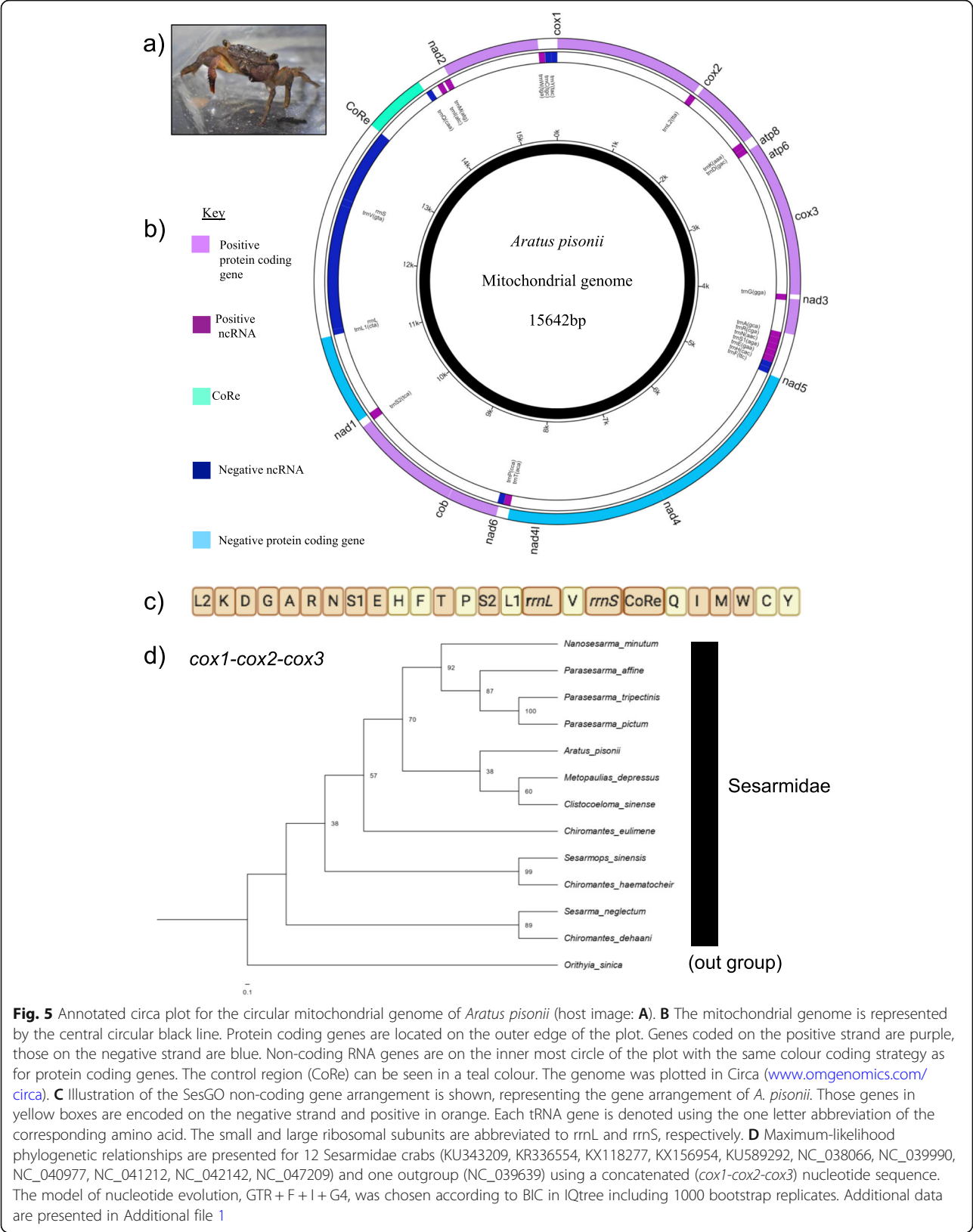


and Mantelatto 2019). We provide histological confirmation of several parasites from a North American (Florida) population, including: a metazoan ectoparasite, a ciliated protozoan, a fungal parasite, and two viral

pathologies. Metagenomic data further identified multiple bacterial species, a novel nudivirus genome, and the presence of a reverse transcribed (complete) *Alphaflexiviridae* genome similar to a strain of CsCMV.

Table 3 Metaxa2 results after mining the metagenomic data for bacterial SSU and LSU sequences

Metagenomic node (length, base pairs) (coverage)	Blastn hit (accession)	Query coverage (%)	Identity (%)	E-value
154,936 (1378) (0.9)	<i>Paracoccus</i> sp. Arc7-R13 (CP034810)	55	88.6	3e-171
199,125 (1237) (1.9)	Bacterial clone (DQ985884)	98	99.9	0.0
346,246 (938) (2.4)	Bacterial clone (FN823684)	100	86.6	0.0
31,499 (2334) (2.1)	Bacterial clone (DQ856534)	100	96.3	0.0
59,853 (1937) (2.0)	Spirochaetes clone (KC990425)	96	88.8	1e-114
64,369 (1892) (3.2)	' <i>Candidatus</i> Gracilibacteria sp.' (CP042461)	43	90.5	0.0
746,052 (504) (1.4)	Bacterial clone (HG792215)	100	99.6	3e-135
7742 (3289) (3.1)	<i>Pseudalteromonas</i> sp. (KF859595)	100	96.5	0.0



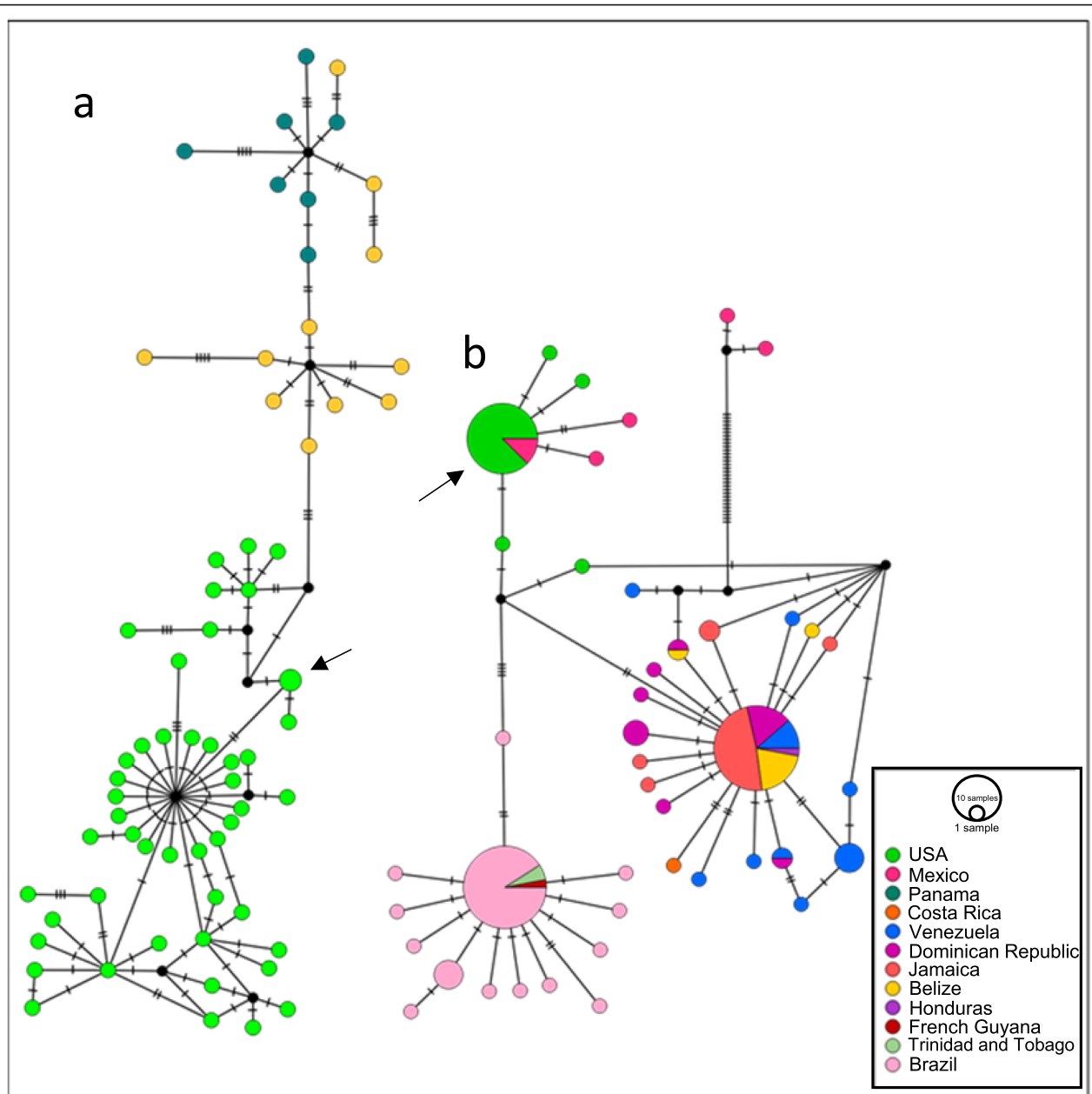


Fig. 6 Two haplotype networks developed using the TCS method in PopArt. The size of each circle is proportional to the frequency of the haplotype. The colour shows the location of where the sequence was obtained. The hatch marks along the lines indicate differences in the nucleotide sequences of the specimens. Black circles indicate missing intermediate haplotypes. **A** 63 CoRe nucleotide sequences from GenBank and the specimen sequenced in this study (total = 64). **B** 133 *cox1* nucleotide sequences from GenBank and the specimen sequenced in this study (total = 134). The specimen sequenced in this study is highlighted using an arrow

The *Aratus pisonii* symbiome

Prior to this study, fungi were the only symbiotic group identified from *A. pisonii* (Mattson 1988). We provide evidence for viral, bacterial, protozoan, and metazoan associations within this host. The Brachyura in general host a diverse array of viruses, spanning both RNA and DNA realms (Bateman and Stentiford 2017; Bojko et al. 2019; Subramaniam et al. 2020). Many of the well-

researched hosts are from marine environments, such as *Carcinus maenas* with over 90 known symbionts (Bojko et al. 2021). A major group of viruses that are gaining greater understanding through metagenomic techniques are the *Nudiviridae* (Allain et al. 2020; Bateman et al. 2021). To date, six crustacean nudivirus genomes have been identified: one from lobster (Holt et al. 2019), three from shrimp (Yang et al. 2014; Bateman et al. 2021), one

from crab (Bateman et al. 2021), and one from an amphipod (Allain et al. 2020). We now provide the seventh crustacean nudivirus from *A. pisonii*, a mangrove crab from the Florida Keys, USA. In each of these hosts, nudiviruses have caused nuclear hypertrophy in hepatopancreatic epithelia, infecting multiple cell-types and often causing cells to slough off into the hepatopancreatic lumen, resulting in degradation of the organ (Bateman et al. 2021). The possible effect for the mangrove crab include the same potential in heavily infected specimens. Since the affected organ functions as a digestive gland for the animal, infection may impede the capacity for digestion of leaf litter and other consumed material.

ApNV shares greatest amino acid similarity with the other crab virus, CmNV. This suggests that the two crab-infecting nudiviruses share a closer evolutionary history relative to other viruses in this group. However, our multi-gene and single-gene phylogenetic analyses suggest that HgNV shares a more similar evolutionary history with CmNV vs ApNV. The three viruses group together with high support, but ApNV is more of an outlier relative to the other two viruses, which group together and have a shorter branch length distance (Fig. 5). CmNV encodes 98 predicted genes and HgNV encodes 97 predicted genes, whereas ApNV encodes fewer predicted genes (91). All three viruses encode all conserved genes for the nudivirus family; however, this difference in number of genes might relate the largest difference between ApNV and the other two most closely related nudiviruses. The missing genes are all hypothetical predicted genes in the other genomes, and their function is unknown. *Aratus pisonii* is a tropical semi-terrestrial species, where both *C. maenas* and *H. gammarus* are cold-water, coastal, European species. These environmental differences may relate to the genomic variation we see between ApNV and CmNV/HgNV. As more crab viruses are sequenced, we may see greater evidence for genome diversity among similar host groups.

Secondly, an alphaflexivirus was identified using the metagenomic approach. An oddity here is that alphaflexiviruses are positive strand RNA viruses (Kreuze et al. 2020) and we identified a DNA genome, suggesting that some reverse transcription may have taken place. The genome we identified was ~98% similar to CsCMV (Collavino et al. 2021). The collected metagenomic data also included a fragment of the Cassava 18S rRNA gene, the plant host of this virus. Together, these data suggest that the discovery of this virus in the crab hepatopancreas may be most likely a result of the Cassava plant identified in the metagenomic data; however, since novel hosts of this virus outside of the plant and whitefly are important to study, we suggest that further work be done to determine if the mangrove crab is a true sink for this virus.

The other groups we identified included bacterial, protozoan, fungal and metazoan symbionts. For the bacteria, taxonomic detail was achieved using a metagenomic approach, which was limited by lack of similar sequences in some cases but allowed for the identification of several genera common to the crustacean gut microbiome (Payne et al. 2008; Tkavc et al. 2011; Chen et al. 2015) or aquatic/terrestrial habitat (Luef et al. 2015). *Paracoccus* sp., '*Candidatus* Gracilibacteria sp.', and *Pseudoalteromonas* sp., were determined to genus level in the *A. pisonii* hepatopancreatic microbiome. The bacterium *Paracoccus* sp. have been associated with pyridine degradation, and the presence of this bacterium may have a mutualistic benefit for the crab host (Wang et al. 2018). Other bacteria in the host microbiome have been found to produce bioactive compounds (e.g. *Pseudoalteromonas* sp.; Bowman 2007), and may also share a mutualistic relationship. The crustacean hepatopancreas is known to host a range of symbiotic or parasitic species and more experimental information would be needed to determine what the role of the above bacteria would be in the *A. pisonii* hepatopancreas (Bojko et al. 2018; Bojko et al. 2022).

The fungus identified in the host testes was not identified to a lower taxon; however, its observation in the gonad of the male host may possibly have resulted in reproductive impairment. The fungus was noted to occupy the entire histological section of testis, and no spermatozoa were observable in the infected organ. We are unfamiliar with other fungal species that parasitise the gonad of crustacean hosts and this may be a relatively novel finding requiring taxonomic detail.

The final two groups, gill protozoans (tentatively Ciliophora) and ectoparasitic metazoans (tentatively Arthropoda) appear more commensal in their symbiotic role with the crab. In all cases the two were not associated with any melanisation or risk to gill structure under histology.

In all, the symbiome of the crab consists of a diverse array of viruses, bacteria, protozoa, fungi, and metazoans, which are likely to impact the health and breeding success of their host. These symbionts are likely to have an impact on the mangrove disease ecology, limiting the population growth of the crab. Further study into the specifics of the disease ecology relationships can now be addressed, using the discoveries presented in this study.

Conclusions

This research have provided the first in-depth exploration of the parasites associated with the mangrove crab *A. pisonii*, increasing the number of known viral, bacterial, protozoan, fungal and metazoan parasites of this host species. The additional host haplotype data, alongside new genetic resources for this host (mitochondrial

genome), reveal a high level of local connectivity between populations in certain regions, but limited connection between others, suggesting that parasite assemblages in one population/location may not be the same relative to other locations that are more distant.

Our description of a novel nudivirus increases the known members of the *Gammanudivirus* genus to seven, providing further taxonomic clarification via multi-gene phylogenetics. In addition, we found a reverse transcribed alphaflexivirus in the pathobiome of this host. Since this virus was detected in a DNA state, it seems unlikely that it was infecting the crab and more likely to be associated with a plant consumed by the crab. The natural host range of CsCMV has not been studied to date, but it is quite plausible the virus infects related species in the family Euphorbiaceae, which may grow in or near mangrove forests. Wild reservoirs of this virus are an important area to study further and this species should be explored using meta-transcriptomic techniques.

Finally, the detailed host haplotype network and discovery of several parasites provide a good foundation for this mangrove crab to become a useful disease ecology model for a semi-marine, semi-terrestrial, tropical species, to understand the role of disease in mangrove ecosystems.

Materials and methods

Collection, identification, and histopathology

Mangrove crabs ($n = 31$), *A. pisonii*, were collected from Long Key, Florida Keys, USA (Lat 24.82°N, Long 80.81°W) in January 2018. A boat was navigated through tight mangrove channels, shaking the trees to knock crabs loose. The animals were anaesthetised prior to dissection by placing into a -20°C freezer for 10 min. A pea-sized amount of hepatopancreas, muscle and gill were also biopsied and submerged in 99% molecular grade ethanol. The same organs with the addition of the gut, gonad, cuticle, and heart were placed into separate labelled cassettes and submerged in Davidson's saltwater fixative for histological analysis.

Davidson's-fixed specimens were given a short decalcification using 'Rapid Decalcifier II' for 20 min before being processed into liquid paraffin wax. The tissues from each cassette were arranged and set into a wax block and left to solidify. Blocks were trimmed and sectioned using a microtome and water bath, allowing the sections to dry onto glass slides prior to staining with haematoxylin and alcoholic eosin and rehydration. The slides were cover slipped, read, and imaged using standard light microscopy and an integrated Leica camera.

Metagenomics

DNA was extracted from a single ethanol-fixed *A. pisonii* hepatopancreas biopsy exhibiting viral infection via

histopathology. Proteinase K in Lifton's Buffer solution was used to digest the ethanol-fixed hepatopancreas, prior to using a Zymo DNA extraction kit following the manufacturers protocol. The DNA extract was frozen at -80°C and then transported on dry ice to Novogene, California, for sequencing. The library was loaded onto an Illumina NovaSeq 6000 using the 150 bp NovaSeq 600 SP reagent kit (300 cycles) for paired-end metagenomic sequencing ($<10\text{Gb}$ of data). The resulting raw reads included 3,007,453 forward and 3,219,600 reverse reads. The raw reads were trimmed and quality checked using Trimmomatic V. 0.36 (LEADING: 3 TRAILING: 3 SLIDINGWINDOW: 4: 15 MINLEN: 36) (Bolger et al. 2014). Assembly was carried out using SPAdes V. 3.15.3 with default parameters (Bankevich et al. 2012), resulting in an N50 of 1162 for the assembled metagenome. This resulted in three complete genomes: a novel member of the *Nudiviridae* (circular, 108,981 bp), a novel *Alphaflexiviridae* strain (linear 6403 bp) and the host mitochondrial genome (circular, 15,642 bp). Genome coverage and continuity was confirmed by mapping all paired and unpaired reads in CLC genomics v.20 (Qiagen).

Further exploration for bacterial and eukaryotic symbionts present in the mangrove crab pathobiome was conducted using Metaxa2 (Bengtsson-Palme et al. 2015). Metaxa2 was applied to the assembled data ($>500\text{ bp}$) to detect the presence of mitochondrial and bacterial SSU and LSU sequences, as well as eukaryotic SSU and LSU sequences. Each sequence was put through NCBItools to check for chimeric sequences, which were removed during submission, and the remaining sequences were compared to existing data on GenBank using BLASTn.

Mitochondrial and viral genome annotation

The mitogenome of the host was collected to provide additional data on host variation and support for future studies exploring this particular species and model disease system. It was annotated using MITOS (Bernt et al. 2013). The location of the *cox1* gene was determined and the genome reorientated with the *cox1* gene at the start of the genome. The annotation was manually checked to identify any obscure elements or mis-annotation via MITOS. The nucleotide and protein similarity data were obtained using BLASTn and BLASTp (NCBI). The nudivirus genome and alphaflexivirus genome were annotated using GeneMarkS (Besemer et al. 2001). The annotated nudivirus and mitochondrial genomes were graphically represented using CIRCA (<http://omgenomics.com/circa/>).

Phylogenetics

Twelve brachyuran *cox1*, *cox2*, and *cox3* sequences were obtained by conducting a BLASTn similarity search to the *A. pisonii* mitogenome nucleotide sequence. The

sequences were trimmed and individually aligned in MAFFT (XSEDE 7.402) available through the CIPRES science gateway (Miller et al. 2012) before being manually concatenated. Maximum-Likelihood (ML) phylogenetic analysis was performed in IQ-Tree, which computed the most appropriate evolutionary model (GTR + F + I + G4) according to Bayesian information criterion (BIC) and 1000 bootstrap replicates (Minh et al. 2015). The resulting tree was annotated using FigTree V. 1.4.3 (<http://tree.bio.ed.ac.uk/software/figtree/>).

A 17-protein ML phylogenetic tree (1000 bootstraps) was inferred from 12 nudivirus genomes and one baculovirus (outgroup). The proteins were aligned separately using MAFFT on CIPRES before combining into a single alignment. The evolutionary model (Q.pfam+F + I + G4) was indicated by BIC during construction of the tree using IQ-Tree. In addition, a second ML tree was developed using the DNA polymerase of each available isolate on GenBank (UBZ25591, YP_010087641, YP_009051843, UHB41724, QLI62362, UBZ25485, YP_009116659, YP_004956766, AAM45757, YP_009553377, YP_001111279, QDF63658, QDF63657, YP_009345924, QHG11240, ABF93350, AKH40386, QDF63651, YP_002321312, QDF63655, QDF63659, QDF63656, QDF63653, YP_009553129, AYP97892, YP_009551711, QKO01844) in addition to that encoded by ApNV. This single-protein tree was also developed using IQ-Tree (1000 bootstraps) (BIC: Q.pfam+F + I + G4).

The novel *Alphaflexiviridae* genome (nucleotide), replicase and capsid proteins were each compared to five available genomes from this species complex (KT002435, U23414, MN243731, MN428639, KT002439) and Turtle Grass X virus (MH077559) (outgroup). The genes were separated into FASTA files and aligned using MAFFT (XSEDE 7.402) (Miller et al. 2012) before conducting Maximum-Likelihood (ML) phylogenetic analysis in IQ-Tree (replicase - 1000 bootstraps, BIC: TN + F + I) (capsid - 1000 bootstraps, BIC: JTT). The resulting trees were annotated using FigTree V. 1.4.3. The whole genome tree was inferred using a neighbour-joining approach in CLC Genomics v.20 (Qiagen). Capsid and replicase amino acid sequences were also compared using the sequence demarcation tool V. 1.2 (Muhire et al. 2014). An alignment of the six Cassava common mosaic virus (CsCMV) genomes was conducted using MUSCLE in CLC Genomics V. 20 (Qiagen), including a similarity colour chart.

Population connectedness for *A. pisonii*

CoRe and *cox1* sequences from *A. pisonii* were obtained from NCBI, GenBank. Sixty-four CoRe sequences and 134 *cox1* sequences were used to generate haplotype networks. The 64 CoRe sequences used (KX096735-KX096739, KX096741-KX096748, KX096750, KX096751, KX096753-

KX096800) are part of PopSet 1,124,070,452, collected by Riley et al. (Riley and Griffen 2017), including specimens from the USA ($n = 45$), Belize ($n = 12$) and Panama ($n = 7$).

The *cox1* sequences for *A. pisonii* (LT626267-LT626360, LT626367-LT626377, LT626380-LT626408) had a broad distribution including the USA ($n = 24$), Mexico ($n = 6$), Brazil ($n = 46$), Venezuela ($n = 15$), Trinidad and Tobago ($n = 2$), Honduras ($n = 1$), Belize ($n = 9$), Costa Rica ($n = 1$), Jamaica ($n = 20$) and Dominican Republic ($n = 9$). Gene-specific Sequences were aligned and trimmed in CLC workbench to the smallest sequence length (804 bp for *cox1* and 442 bp for CoRe). The trimmed sequences were aligned in MAFFT (XSEDE V. 7.402) via CIPRES (Miller et al. 2012). Haplotype networks were constructed using the TCS network method in PopArt V. 1.7.2. (Leigh and Bryant 2015).

Abbreviations

ApNV: *Aratus pisonii* nudivirus; CmNV: *Carcinus maenas* nudivirus; HgNV: *Homarus gammarus* nudivirus; PmNV: *Penaeus monodon* nudivirus; MrNV: *Macrobrachium rosenbergii* nudivirus; DhNV: *Dikerogammarus haemobaphes* nudivirus; CsCMV: Cassava common mosaic virus; CoRe: Mitochondrial core region

Supplementary Information

The online version contains supplementary material available at <https://doi.org/10.1186/s44149-022-00039-7>.

Additional file 1: Table S1. Data acquired from BLASTn shows the nucleotide similarity for protein coding and non-coding genes of the *Aratus pisonii* mitochondrial genome. The accession number for the nucleotide sequence are provided, alongside the species name. The percentage similarity, coverage and e-value are provided. Underlined gene names indicates the gene is coded on the negative strand. **Table S2.** Data acquired from BLASTp shows the protein similarity of the amino acid sequences encoded by *Aratus pisonii* mitochondrial genome. The accession number for the protein sequence are provided, alongside the species name. The percentage similarity, coverage and e-value are provided. Underlined gene names indicates the gene is coded on the negative strand.

Acknowledgements

The authors would like to thank Mr. Lucas Jennings for taxonomic confirmation of the crab specimens and Mr. Nate Berkebile (FWC) for help when collecting the specimens.

Authors' contributions

JB conceived the project with DCB, JB, EPR and DP collected the animals and conducted dissections. JB conducted histological analysis. ALB and JB conducted the mitochondrial genomics and haplotype analysis. JB, JFK, TWA and ALB conducted viral assembly and phylogenetic analysis. JB, ALB, TWA, EPR, DP, JFK, and DCB all contributed to the writing and synthesis of the manuscript text. The author(s) read and approved the final manuscript.

Funding

JB and DCB would like to acknowledge personal research funds at Teesside University and the University of Florida, which were used to support this project. ALB would like to acknowledge PhD research funding attained from Teesside University.

Availability of data and materials

The dataset(s) supporting the conclusions of this article are available from the NCBI repository, under accession numbers: ON061174, OM927720, ON063416-ON063422.

Declarations

Ethics approval and consent to participate

All specimens used in this study were invertebrate animals.

Consent for publication

All authors consent to publication of this manuscript.

Competing interests

The authors declare that they have no competing interests.

Author details

¹National Horizons Centre, Teesside University, Darlington DL1 1HG, UK. ²School of Health and Life Sciences, Teesside University, Middlesbrough TS1 3BX, UK. ³Fisheries and Aquatic Sciences, University of Florida, Gainesville, FL 32653, USA. ⁴Emerging Pathogens Institute, University of Florida, Gainesville, FL 32611, USA. ⁵Florida Fish and Wildlife Research Institute, Marathon, FL 33050, USA. ⁶International Potato Centre (CIP), Apartado 1558, Lima, Peru.

Received: 26 March 2022 Accepted: 8 April 2022

Published online: 05 May 2022

References

- Allain, T.W., G.D. Stentiford, D. Bass, D.C. Behringer, and J. Bojko. 2020. A novel nudivirus infecting the invasive demon shrimp *Dikerogammarus haemobaphes* (Amphipoda). *Scientific Reports* 10 (1): 1–13. <https://doi.org/10.1038/s41598-020-71776-3>.
- Bankevich, A., S. Nurk, D. Antipov, A.A. Gurevich, M. Dvorkin, A.S. Kulikov, V.M. Lesin, S.I. Nikolenko, S. Pham, A.D. Pribelski, A.V. Pyshkin, A.V. Sirotkin, N. Vyahhi, G. Tesler, M.A. Alekseyev, and P.A. Pevzner. 2012. SPAdes: A new genome assembly algorithm and its applications to single-cell sequencing. *Journal of Computational Biology* 19 (5): 455–477. <https://doi.org/10.1089/cmb.2012.0021>.
- Bass, D., G.D. Stentiford, H.C. Wang, B. Koskella, and C.R. Tyler. 2019. The pathobiome in animal and plant diseases. *Trends in Ecology & Evolution* 34 (11): 996–1008. <https://doi.org/10.1016/j.tree.2019.07.012>.
- Basso, A., M. Babbucci, M. Pauletto, E. Riginella, T. Patarnello, and E. Negrisolo. 2017. The highly rearranged mitochondrial genomes of the crabs *Maja craspata* and *Maja squinado* (Majidae) and gene order evolution in Brachyura. *Scientific Reports* 7 (1): 1–17. <https://doi.org/10.1038/s41598-017-04168-9>.
- Bateman, K.S., R. Kerr, G.D. Stentiford, T.P. Bean, C. Hooper, B. van Eynde, D. Delbare, J. Bojko, O. Christiaens, C.N.T. Tanning, G. Smagghe, M.M. van Oers, and R. van Aerle. 2021. Identification and full characterisation of two novel crustacean infecting members of the family Nudiviridae provides support for two subfamilies. *Viruses* 13 (9): 1694. <https://doi.org/10.3390/v13091694>.
- Bateman, K.S., and G.D. Stentiford. 2017. A taxonomic review of viruses infecting crustaceans with an emphasis on wild hosts. *Journal of Invertebrate Pathology* 147: 86–110. <https://doi.org/10.1016/j.jip.2017.01.010>.
- Behrens, M.D., and K.D. Lafferty. 2004. Effects of marine reserves and urchin disease on southern Californian rocky reef communities. *Marine Ecology Progress Series* 279: 129–139. <https://doi.org/10.3354/meps279129>.
- Bengtsson-Palme, J., M. Hartmann, K.M. Eriksson, C. Pal, K. Thorell, D.G.J. Larsson, and R.H. Nilsson. 2015. METAXA2: Improved identification and taxonomic classification of small and large subunit rRNA in metagenomic data. *Molecular Ecology Resources* 15 (6): 1403–1414. <https://doi.org/10.1111/1755-0998.12399>.
- Bernt, M., A. Donath, F. Jühling, F. Externbrink, C. Florentz, G. Fritzsch, J. Pütz, M. Middendorf, and P.F. Stadler. 2013. MITOS: improved de novo metazoan mitochondrial genome annotation. *Molecular Phylogenetics and Evolution* 69 (2): 313–319. <https://doi.org/10.1016/j.ympev.2012.08.023>.
- Besemer, J., A. Lomsadze, and M. Borodovsky. 2001. GeneMarkS: A self-training method for prediction of gene starts in microbial genomes. Implications for finding sequence motifs in regulatory regions. *Nucleic Acids Research* 29 (12): 2607–2618. <https://doi.org/10.1093/nar/29.12.2607>.
- Bojko, J., K. Bączela-Spychalska, P.D. Stebbing, A.M. Dunn, M. Grabowski, M. Rachalewski, and G.D. Stentiford. 2017. Parasites, pathogens, and commensals in the “low-impact” non-native amphipod host *Gammarus roeselii*. *Parasites & Vectors* 10 (1): 1–15. <https://doi.org/10.1186/s13071-017-2108-6>.
- Bojko, J., A.L. Burgess, A.G. Baker, and C.H. Orr. 2021. Invasive non-native crustacean symbionts: Diversity and impact. *Journal of Invertebrate Pathology* 186: 107482. <https://doi.org/10.1016/j.jip.2020.107482>.
- Bojko, J., A.M. Dunn, P.D. Stebbing, R. van Aerle, K. Bączela-Spychalska, T.P. Bean, A. Urrutia, and G.D. Stentiford. 2018. ‘*Candidatus* Aquirickettsiella gammari’ (Gammaproteobacteria: Legionellales: Coxiellaceae): A bacterial pathogen of the freshwater crustacean *Gammarus fossarum* (Malacostraca: Amphipoda). *Journal of Invertebrate Pathology* 156: 41–53. <https://doi.org/10.1016/j.jip.2018.07.010>.
- Bojko, J., K. McCoy, and A. Blakeslee. 2022. ‘*Candidatus* Mellornella promiscua’ n. gen. n. sp. (Alphaproteobacteria: Rickettsiales: Anaplasmataceae): an intracytoplasmic, hepatopancreatic, pathogen of the flatback mud crab, *Eurypanopeus depressus*. *Journal of Invertebrate Pathology* 190: 107737.
- Bojko, J., K. Subramaniam, T.B. Waltzek, G.D. Stentiford, and D.C. Behringer. 2019. Genomic and developmental characterisation of a novel bunyavirus infecting the crustacean *Carcinus maenas*. *Scientific Reports* 9 (1): 1–10. <https://doi.org/10.1038/s41598-019-49260-4>.
- Bolger, A.M., M. Lohse, and B. Usadel. 2014. Trimmomatic: A flexible trimmer for Illumina sequence data. *Bioinformatics* 30 (15): 2114–2120. <https://doi.org/10.1093/bioinformatics/btu170>.
- Bowman, J.P. 2007. Bioactive compound synthetic capacity and ecological significance of marine bacterial genus *Pseudoalteromonas*. *Marine Drugs* 5 (4): 220–241. <https://doi.org/10.3390/md504220>.
- Buranelli, R.C., and F.L. Mantelatto. 2019. Comparative genetic differentiation study of three coexisting mangrove crabs in western Atlantic. *Journal of Natural History* 53 (47–48): 2883–2903. <https://doi.org/10.1080/00222933.2020.1751889>.
- Chen, X., P. Di, H. Wang, et al. 2015. Bacterial community associated with the intestinal tract of Chinese mitten crab (*Eriocheir sinensis*) farmed in Lake tai, China. *PLoS One* 10 (4): e0123990. <https://doi.org/10.1371/journal.pone.0123990>.
- Collavino, A., A.A. Zanini, R. Medina, S. Schaller, and L. di Feo. 2021. Cassava common mosaic virus infection affects growth and yield components of cassava plants (*Manihot esculenta*) in Argentina. *Plant Pathology*. <https://doi.org/10.1111/ppa.13515>.
- Conde, J.E., M.M.P. Tognella, E.T. Paes, et al. 2000. Population and life history features of the crab *Aratus pisonii* (Decapoda: Grapsidae) in a subtropical estuary. *Interciencia* 25: 151–158.
- Díaz, H., and J.E. Conde. 1989. Population dynamics and life history of the mangrove crab *Aratus pisonii* (Brachyura, Grapsidae) in a marine environment. *Bulletin of Marine Science* 45: 148–163.
- Holt, C.C., M. Stone, D. Bass, et al. 2019. The first clawed lobster virus *Homarus gammarus* nudivirus (HgNV n. sp.) expands the diversity of the *Nudiviridae*. *Scientific Reports* 9: 1–15.
- Kreuze, J.F., A.M. Vaira, W. Menzel, T. Candresse, S.K. Zavriev, J. Hammond, K. Hyun Ryu, and I.C.T.V. Report Consortium. 2020. ICTV virus taxonomy profile: *Alphaflexiviridae*. *The Journal of General Virology* 101 (7): 699–700. <https://doi.org/10.1099/jgv.0.001436>.
- Leigh, J.W., and D. Bryant. 2015. POPART: Full-feature software for haplotype network construction. *Methods in Ecology and Evolution* 6 (9): 1110–1116. <https://doi.org/10.1111/2041-210X.12410>.
- Luef, B., K.R. Frischkorn, K.C. Wrigton, H.Y.N. Holman, G. Birarda, B.C. Thomas, A. Singh, K.H. Williams, C.E. Siegerist, S.G. Tringe, K.H. Downing, L.R. Comolli, and J.F. Banfield. 2015. Diverse uncultivated ultra-small bacterial cells in groundwater. *Nature Communications* 6 (1): 1–8. <https://doi.org/10.1038/ncomms7372>.
- Mattson, R.A. 1988. Occurrence and abundance of eccrinaceous fungi (Trichomycetes) in brachyuran crabs from Tampa Bay, Florida. *Journal of Crustacean Biology* 8 (1): 20–30. <https://doi.org/10.2307/1548426>.
- Miller, M.A., W. Pfeiffer, and T. Schwartz. 2012. The CIPRES science gateway: enabling high-impact science for phylogenetics researchers with limited resources. In *Proceedings of the 1st Conference of the Extreme Science and Engineering Discovery Environment: Bridging from the extreme to the campus and beyond*, 1–8. https://dl.acm.org/doi/abs/10.1145/2335755.2335836?casa_token=Ukd1YpLDw68AAAAA:AoPLhnO6aWQjYfYMC1tXy1G14rAJHdt6NFs50EvVeFJqDSAYvZpFFY8tmXbYij_t1Lp2_o4jg3FfbqRY.
- Minh, B.Q., L.T. Nguyen, H.A. Schmidt, and A. Von Haeseler. 2015. IQ-TREE: a fast and effective stochastic algorithm for estimating maximum-likelihood phylogenies. *Molecular biology and evolution* 32 (1): 268–274.

- Muhire, B.M., A. Varsani, and D.P. Martin. 2014. SDT: A virus classification tool based on pairwise sequence alignment and identity calculation. *PLoS One* 9 (9): e108277. <https://doi.org/10.1371/journal.pone.0108277>.
- Payne, M.S., L. Høj, M. Wietz, et al. 2008. Microbial diversity of mid-stage *Palinurid* phyllosoma from great barrier reef waters. *Journal of Applied Microbiology* 105 (2): 340–350. <https://doi.org/10.1111/j.1365-2672.2008.03749.x>.
- Riley, M.E., and B.D. Griffen. 2017. Habitat-specific differences alter traditional biogeographic patterns of life history in a climate-change induced range expansion. *PLoS One* 12 (5): e0176263. <https://doi.org/10.1371/journal.pone.0176263>.
- Riley, M.E., C.A. Johnston, I.C. Feller, and B.D. Griffen. 2014. Range expansion of *Aratus pisonii* (mangrove tree crab) into novel vegetative habitats. *Southeastern Naturalist* 13 (4): N43–N48. <https://doi.org/10.1656/058.013.0405>.
- Rogers, M.S.J., M. Bithell, S.M. Brooks, and T. Spencer. 2021. VEdge_Detector: Automated coastal vegetation edge detection using a convolutional neural network. *International Journal of Remote Sensing* 42 (13): 4805–4835. <https://doi.org/10.1080/01431161.2021.1897185>.
- Sandilyan, S., and K. Kathiresan. 2012. Mangrove conservation: A global perspective. *Biodiversity and Conservation* 21 (14): 3523–3542. <https://doi.org/10.1007/s10531-012-0388-x>.
- Smith, T.J., III, K.G. Boto, S.D. Frusher, and R.L. Giddins. 1991. Keystone species and mangrove forest dynamics: The influence of burrowing by crabs on soil nutrient status and forest productivity. *Estuarine, Coastal and Shelf Science* 33 (5): 419–432. [https://doi.org/10.1016/0272-7714\(91\)90081-L](https://doi.org/10.1016/0272-7714(91)90081-L).
- Strauss, A.T., L.G. Shoemaker, E.W. Seabloom, and E.T. Borer. 2019. Cross-scale dynamics in community and disease ecology: Relative timescales shape the community ecology of pathogens. *Ecology* 100 (11): e02836. <https://doi.org/10.1002/ecs.2836>.
- Subramaniam, K., D.C. Behringer, J. Bojko, et al. 2020. A new family of DNA viruses causing disease in crustaceans from diverse aquatic biomes. *MBio* 11: e02938–e02919.
- Tkavc, R., L. Ausec, A. Oren, and N. Gunde-Cimerman. 2011. Bacteria associated with *Artemia* spp. along the salinity gradient of the solar salterns at Eilat (Israel). *FEMS Microbiology Ecology* 77 (2): 310–321. <https://doi.org/10.1111/j.1574-6941.2011.01112.x>.
- Wang, J., X. Jiang, X. Liu, X. Sun, W. Han, J. Li, L. Wang, and J. Shen. 2018. Microbial degradation mechanism of pyridine by *Paracoccus* sp. NJUST30 newly isolated from aerobic granules. *Chemical Engineering Journal* 344: 86–94. <https://doi.org/10.1016/j.cej.2018.03.059>.
- Warren, D.A., A.L. Burgess, F. Karemera, K. Bacela-Spychalska, G.D. Stentiford, and J. Bojko. 2022. Histopathological survey for parasite groups in *Gammarus varsoviensis* (Amphipoda). *Diseases of Aquatic Organisms*, In Press. <https://doi.org/10.3354/dao03658>.
- Yang, Y.T., D.Y. Lee, Y. Wang, et al. 2014. The genome and occlusion bodies of marine *Penaeus monodon* nudivirus (PmNV, also known as MBV and PemoNPV) suggest that it should be assigned to a new nudivirus genus that is distinct from the terrestrial nudiviruses. *BMC Genomics* 15: 1–24.

Publisher's Note

Springer Nature remains neutral with regard to jurisdictional claims in published maps and institutional affiliations.

Ready to submit your research? Choose BMC and benefit from:

- fast, convenient online submission
- thorough peer review by experienced researchers in your field
- rapid publication on acceptance
- support for research data, including large and complex data types
- gold Open Access which fosters wider collaboration and increased citations
- maximum visibility for your research: over 100M website views per year

At BMC, research is always in progress.

Learn more biomedcentral.com/submissions

